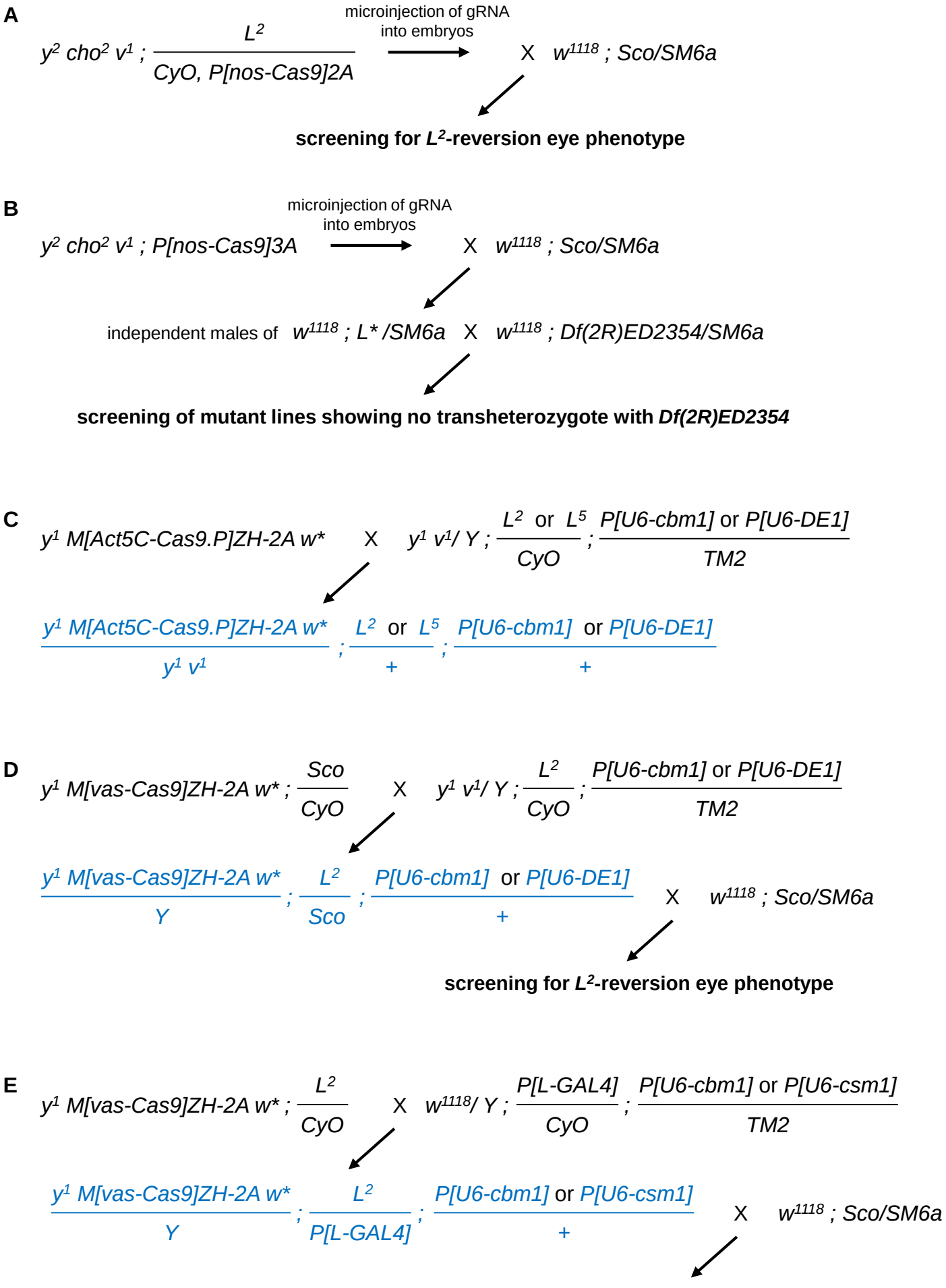
A
y2 cho2 v1 ; L2 / CyO, P[nos-Cas9]2A
microinjection of gRNA into embryos
X w1118 ; Sco/SM6a
screening for L2-reversion eye phenotype
B
y2 cho2 v1 ; P[nos-Cas9]3A
microinjection of gRNA into embryos
X w1118 ; Sco/SM6a
independent males of w1118 ; L* /SM6a X w1118 ; Df(2R)ED2354/SM6a
screening of mutant lines showing no transheterozygote with Df(2R)ED2354
C
y1 M[Act5C-Cas9.P]ZH-2A w* X y1 v1/ Y ; L2 or L5 / CyO ; P[U6-cbm1] or P[U6-DE1] / TM2
y1 M[Act5C-Cas9.P]ZH-2A w* / y1 v1 ; L2 or L5 / + ; P[U6-cbm1] or P[U6-DE1] / +
D
y1 M[vas-Cas9]ZH-2A w* ; Sco / CyO X y1 v1/ Y ; L2 / CyO ; P[U6-cbm1] or P[U6-DE1] / TM2
y1 M[vas-Cas9]ZH-2A w* / Y ; L2 / Sco ; P[U6-cbm1] or P[U6-DE1] / + X w1118 ; Sco/SM6a
screening for L2-reversion eye phenotype
E
y1 M[vas-Cas9]ZH-2A w* ; L2 / CyO X w1118/ Y ; P[L-GAL4] / CyO ; P[U6-cbm1] or P[U6-csm1] / TM2
y1 M[vas-Cas9]ZH-2A w* / Y ; L2 / P[L-GAL4] ; P[U6-cbm1] or P[U6-csm1] / + X w1118 ; Sco/SM6a
screening for recombination of L2 (or modified L2) and w+m phenotypes

Figure S1. Genetic schemes for CRISPR mutagenesis in the *L* region.

(A, B) *L* loss-of-function mutants, L^{D0B}, L^{gR1}, and L^{P3}, were generated by microinjection of gRNA vectors into L^{2} or wild-type embryos expressing Cas9 in the germline, and screened for reversion of the L^{2}/+ eye phenotype (A) or complementation failure over a *L*-uncovering deficiency (B). (C) Somatic targeting to modify L^{2}/+ or L^{5}/+ eye phenotypes. Variegated *L* eye phenotypes were examined among the F1 progeny (blue). (D) Germline targeting of L^{2} at *L-RB* specific sequences or flanking sequences of *opus[ ]Mohr*. F2 progeny from the mutagenic F1 males (blue) was screened for modified eye phenotypes. (E) Targeted recombination between L^{2} and *L-GAL4* insertions (*P[GawB]NP5288* and *P[GawB]GH146*, Figure 4B). F2 progeny from the mutagenic F1 males (blue) was screened for recombination of both dominant eye phenotypes (parental or modified *L* eye and w^{+m} expression).

w^{1118}

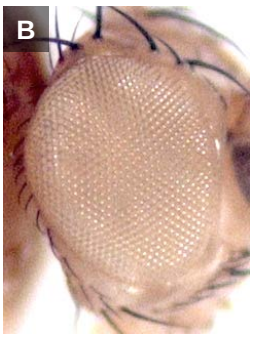

P17/P17

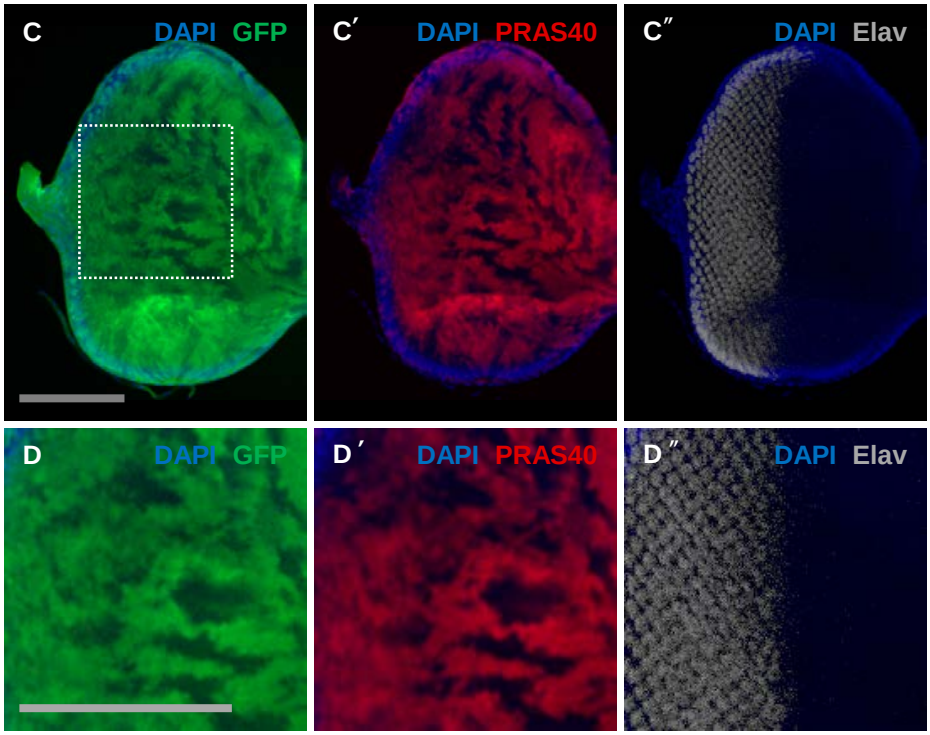

ey-FLP / Ubx-FLP; FRT42D ubi-GFP / FRT42D P17

ey>PRAS40

ey>PRAS40, P17/+

ey>PRAS40,
>PRAS40 RNAi

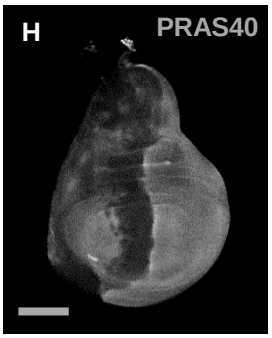

ptc>PRAS40 RNAi

w^{1118}; L^2/+

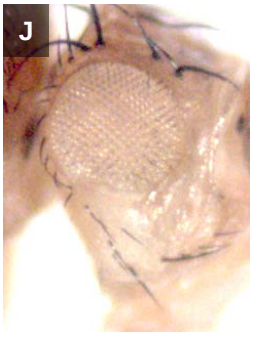

w^{1118}; L^2/P17

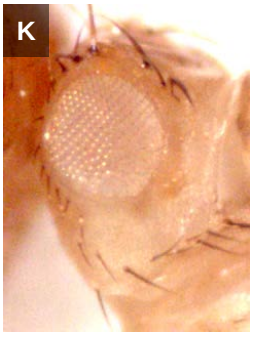

y^1 w^*; L^2/+

y^1 w^*; L^2/$PRAS40^{KO}$

Figure S2. *P17* is a loss-of-function mutant of *PRAS40*.

(A, B) The lethality of *P17* was removed by backcrossing with L^2 or a *L*-uncovering deficiency (*Df(2R)ED2354*) that had been backcrossed with an isogenic control strain (RYDER *et al.* 2004). The *P17* homozygotes show normal eye development (B). (C) *P17* clones in eye discs showed no PRAS40 staining (C') but a normal pattern of Elav staining (C"). The boxed areas in (C) are enlarged in (D-D"). (E-H) The genetic relationship between *P17* stock and *PRAS40.* Eye reduction by *PRAS40* overexpression (E). *P17/+* suppresses the *ey>PRAS40* phenotype (F). *PRAS40 RNAi* fully suppresses *ey>PRAS40* phenotype (G). (H) *PRAS40 RNAi* by *ptc-GAL4* shows knockdown of PRAS40 protein expression in the *ptc* domain. (I-L) Genetic interaction of L^2 and *P17* or $PRAS40^{KO}$ mutation. However, L^2/+ phenotype (I, K) is not affected by *P17/+* (J)or $PRAS40^{KO}$/+ (L).

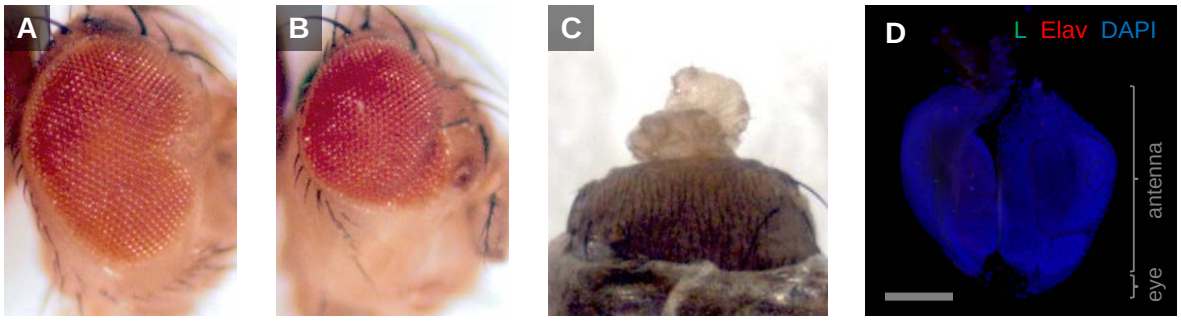

ey-GAL4/ P[XP]d09084

ey-GAL4/ P[XP]d09084

ey-GAL4/ P[GSV1]s-72

ey-GAL4/ P[GSV1]s-72

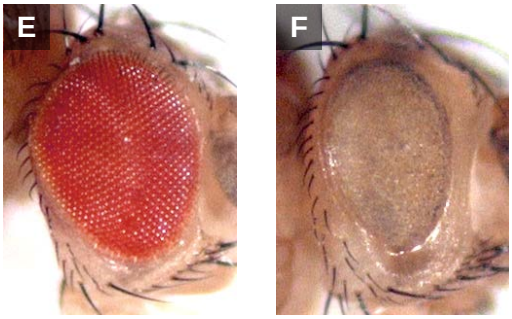

GMR-GAL4/ P[XP]d09084

GMR-GAL4/ P[GSV1]s-72

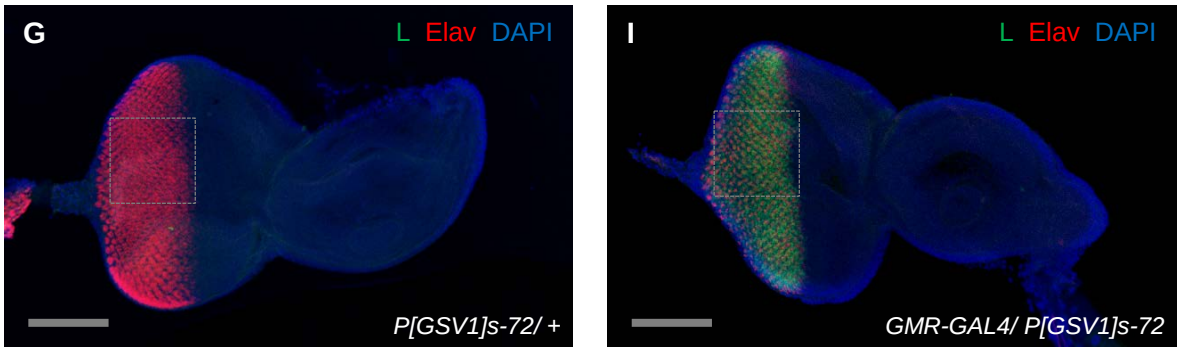

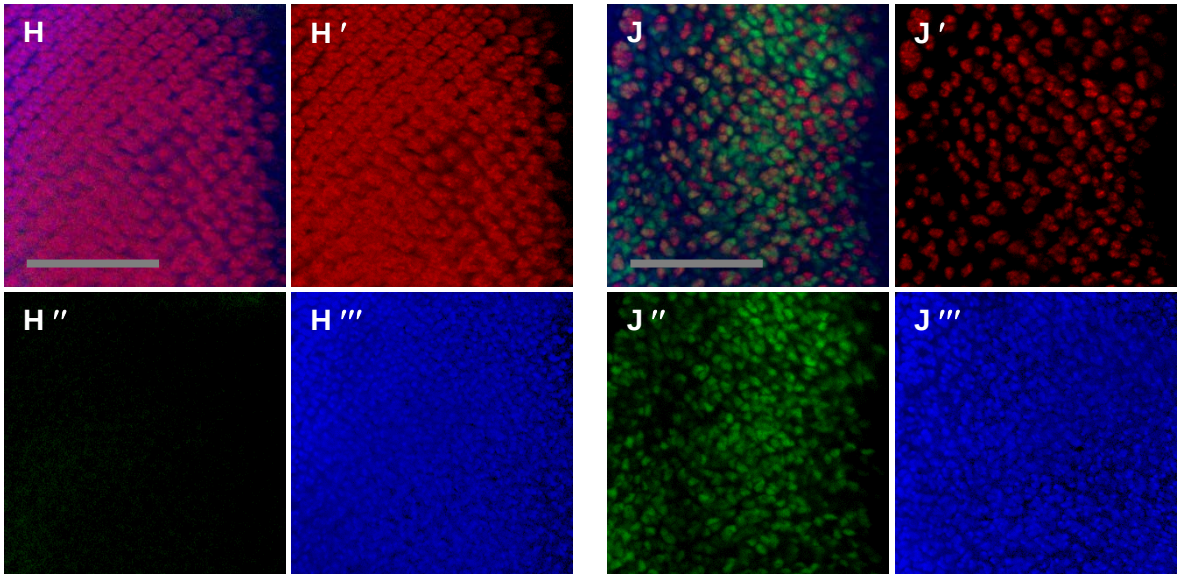

Figure S3. Effects of ectopic *L* expression in the eye.

(A-D) Effects of ectopic *L* expression by two *L* EP lines in the eye. *L* expression by *P[XP]d09084* generated viable offspring with variable eye defects (A, B). *ey-GAL4/P[GSV1]s-72* resulted in lethal pupae that have only antennal and mouth parts left in the head (C). Third instar larval eye-antenna discs of *ey-GAL4/P[GSV1]s-72* showed loss of most *ey-GAL4*-expressing part (D), consistent with ectopic cell death in dominant *L* eyes (SINGH *et al.* 2006). (E-J) *L* expression during retinal differentiation caused a relatively mild reduction in eye size but the ommatidial pattern was lost, resulting in a glossy eye surface. Larval eye discs showed loss of Elav expression in many photoreceptor precursor cells (I, J). Boxed areas in (G, I) are enlarged in (H, J), respectively. Images were taken at 100X magnification (G, I), or at 400X magnification (H, J). Scale bars are 100 μm in (D, G, I) and 50 μm in (H, J).

A

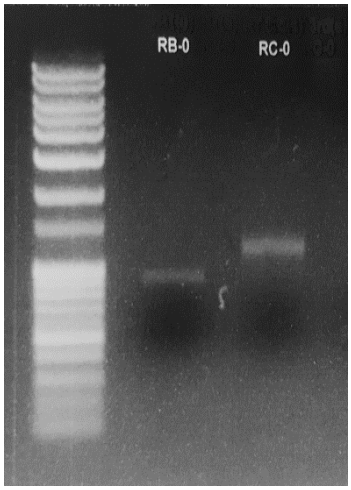

B

```
L-PC        MSRRKQAKPRACLKLGE-KEDEENTGLL----------EPKEELLSG--------DEDNEDNEGEDEDEEVADEVA-

X.Zfp521    MSRRKQAKPR-SLKDPNCKL-EDTS------------EDGESPDCKKRQ-----------EEGDELEEEE---AV-
r.Zfp521    MSRRKQAKPR-SLKDPNCKL-EDKI------------EDGEAVDCKKRP-----------DDGEELEED----AV-
m.Zfp521    MSRRKQAKPR-SLKDPNCKL-EDKI------------EDGEAVDCKKRP-----------EDGEELEED----AV-
h.ZNF521    MSRRKQAKPR-SLKDPNCKL-EDKT------------EDGEALDCKKRP-----------EDGEELEDE----AV-

X.Zfp423    MSRRKQAKPR-SVKVEDA---EDFGLNWESTVNQTGGLDRETDGEGQT---LEDGNSMTSQEERIEEEE-LEDESI-
r.Zfp423    MSRRKQAKPR-SVKVEEGEA-SDFSLAWDSSVAAAGGLEGESECDRKSSRALEDRNSVTSQEERNEDDEDVEDESI-
m.Zfp423    MSRRKQAKPR-SVKVEEGEA-SDFSLAWDSSVAAAGGLEGEPECDRKTSRALEDRNSVTSQEERNEDDEDVEDESI-
h.ZNF423    MHKKR---------VEEGEA-SDFSLAWDSSVTAAGGLEGEPECDQKTSRALEDRNSVTSQEERNEDDEDMEDESI-

Fog-1,-2    MSPRKQSxPR-QIKRxLxxxxxxE(E/D)
```

Figure S4. Identification of *L* transcripts and sequence comparison of Zfp423 family proteins.

(A) RT-PCR of *L* transcript from *CS* wild-type embryos. The transcription level of endogenous *L* was very low, so that *L-RB* and *L-RC* expressions were visible after the second and third nested PCR, respectively. Sequences of the PCR products corresponded to the predicted sequences available in FlyBase except for a few polymorphisms. Primers for the final nested PCRs are; 5'-atgatggccctaaagatgttatatcgtggtcccagttcg-3' and 5'-ccgaacccgtggaccgcggactatagttgag-3' for the 5' terminus of *L-RB* CDS (RB-0, 856 bp PCR product from *L-RB* exon 1 to 4); and 5'-atgtcccgacgcaaacaggccaagccgc-3' and 5'- ccgaacccgtggaccgcggactatagttgag-3' for the 5' terminus of *L-RC* CDS (RC-0, 1270 bp PCR product from *L-RC* exon 1 to 6). (B) Sequence alignments of N-termini of the L-PC splice form and the vertebrate Zfp423 family factors. The L-PC shows a conserved NuRD motif that is followed by ED-rich sequences. The L-PB splice form lacks this motif (Figure 4). Consensus residues in the NuRD motif are indicated by a gray background. The blue underline in the L-PC sequence corresponds to the first exon of *L-RC*. The listed vertebrate Zfp423 family proteins are from *Xenopus* to human (*X*, *Xenopus laevis*; r, rat; m, mouse; h, human). Fog-1 and Fog-2 consensus residues of the NuRD motif are determined by sequence alignment of the vertebrate proteins (LIN *et al.* 2004; HONG *et al.* 2005).

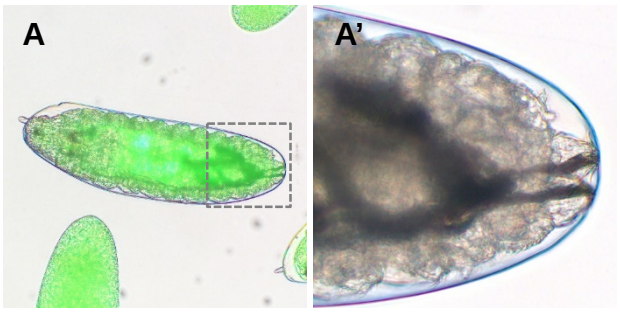

L^{gR1}/ CyO,Act-GFP

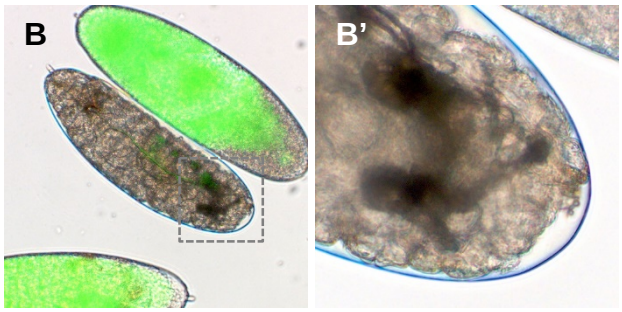

L^{gR1}/ L^{gR1}

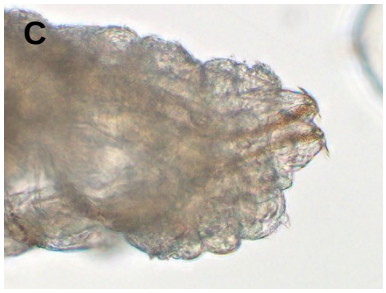

L^{rev6-3}/ CyO,Act-GFP

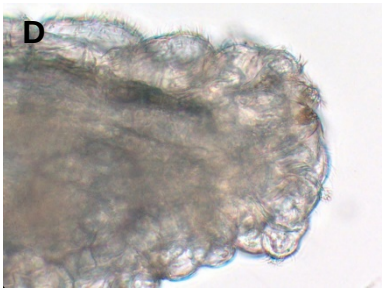

L^{rev6-3}/ L^{gR1}

L^{gR1}/ CyO,Act-GFP

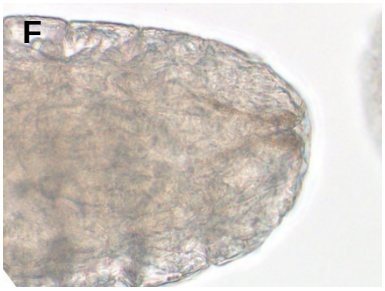

L^{gR1}/ L^{gR1}

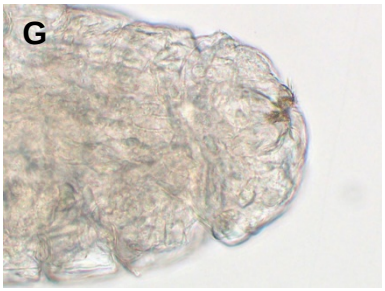

L^{P3}/ L^{P3}

Figure S5. Developmental defects in embryonic and larval posterior spiracles of *L* loss-of-function mutants.

Posterior spiracles were examined in $L^{rev6\text{-}3}$ and newly isolated lethal *L* mutants. (A, B) When compared to L^{gR1}/+ heterozygotes (GFP-positive) that showed normal posterior spiracles, late embryos of the homozygous L^{gR1} (GFP-negative) featured reduced protrusion of the posterior part. Boxed areas in A and B are magnified in A' and B', respectively. (C-G) Posterior defects in the first instar larvae. Heterozygote controls $L^{rev6\text{-}3}$/*CyO* (C) and L^{gR1}/*CyO* show normal posterior structure. Severe posterior defects are seen in escaper larvae from $L^{rev6\text{-}3}$/ L^{gR1} transheterozygotes (D) and homozygotes for L^{gR1} (F) or L^{P3} (G).

A *Act-Cas9/+; L^2/+*

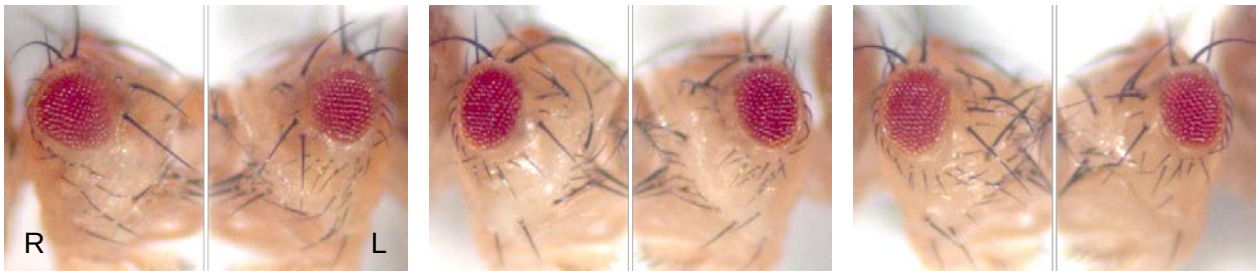

B *Act-Cas9/+; L^2/+; U6-cbm1/+*

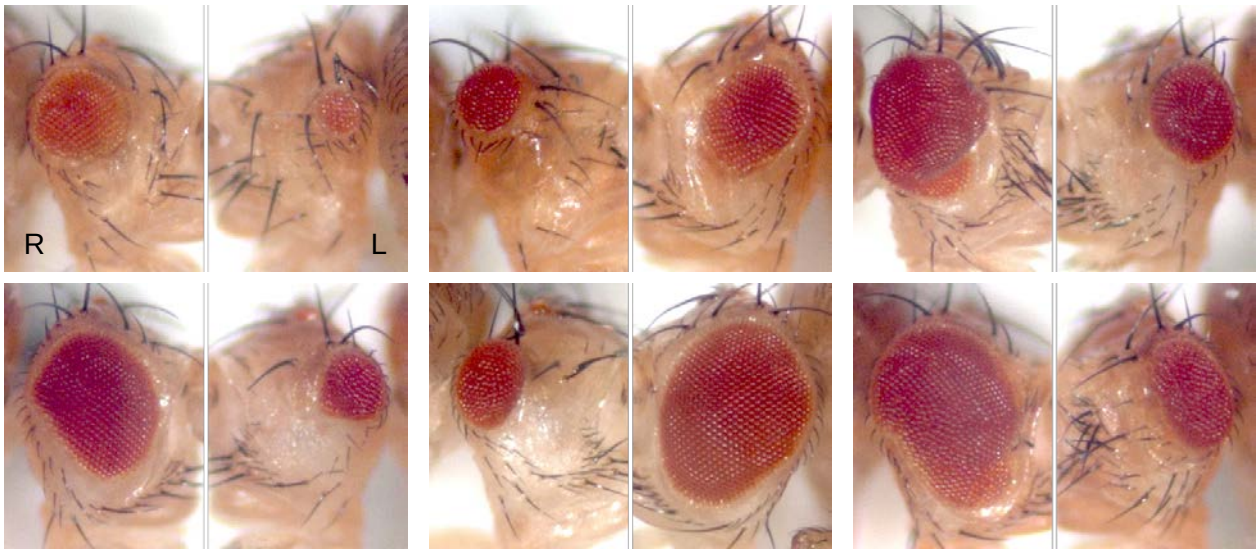

C *Act-Cas9/+; L^2/+; U6-DE1/+*

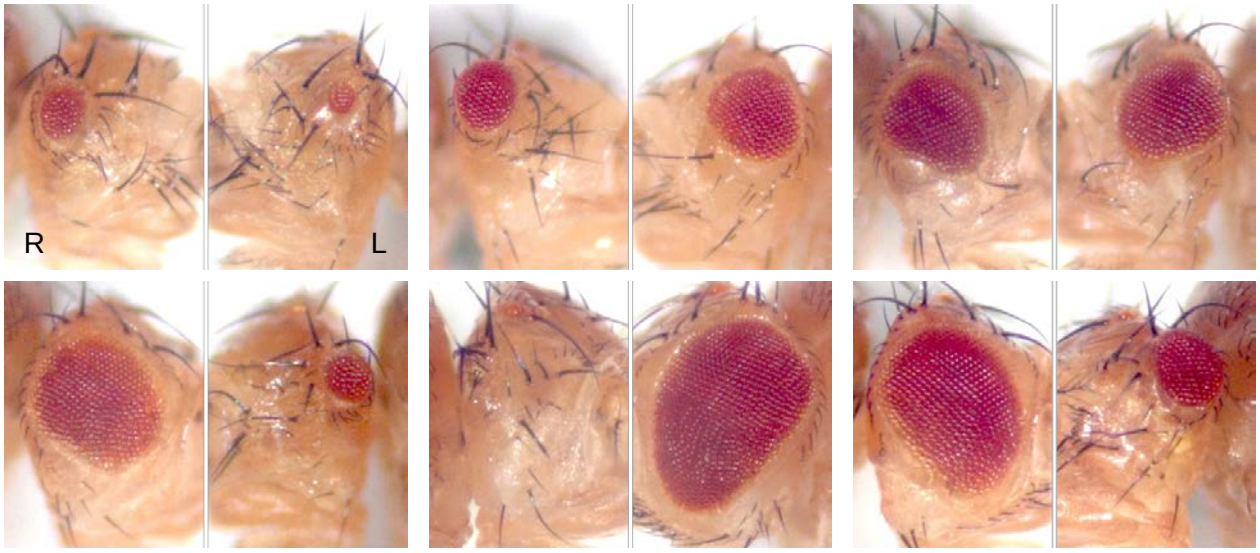

Figure S6. Suppression of *L^2* eye phenotype by somatic CRISPR targeting.

Suppression of *L^2* eye phenotype by somatic CRISPR targeting with ubiquitous *Cas9* expression. The CRISPR targets of *U6-cbm1* are within the *L-RB*-specific transcription unit, and targets of *U6-DE1* are located in both sides flanking *opus[ ]Mohr*. These gRNA transgenic flies were crossed to the ubiquitous *Act-Cas9* to induce suppression of *L^2*/+ eye phenotype by somatic targeting. (A) In the absence of gRNA transgenes (*Act-Cas9/+; L^2*/+), the *L^2*/+ eye phenotype is not modified. (B, C) In the presence of gRNAs, *Act-Cas9/+; L^2*/+*; U6-cbm1*/+ (B) or *Act-Cas9/+; L^2*/+*; U6-DE1*/+ (C), *L^2*/+ eye phenotype is variably suppressed in genetically mosaic eyes induced by somatic targeting. The variegated *L^2*/+ eye phenotypes were detected in 60-70 % of F1 progenies (n>100). Both left and right eyes of each individuals are presented to show phenotypic variation.

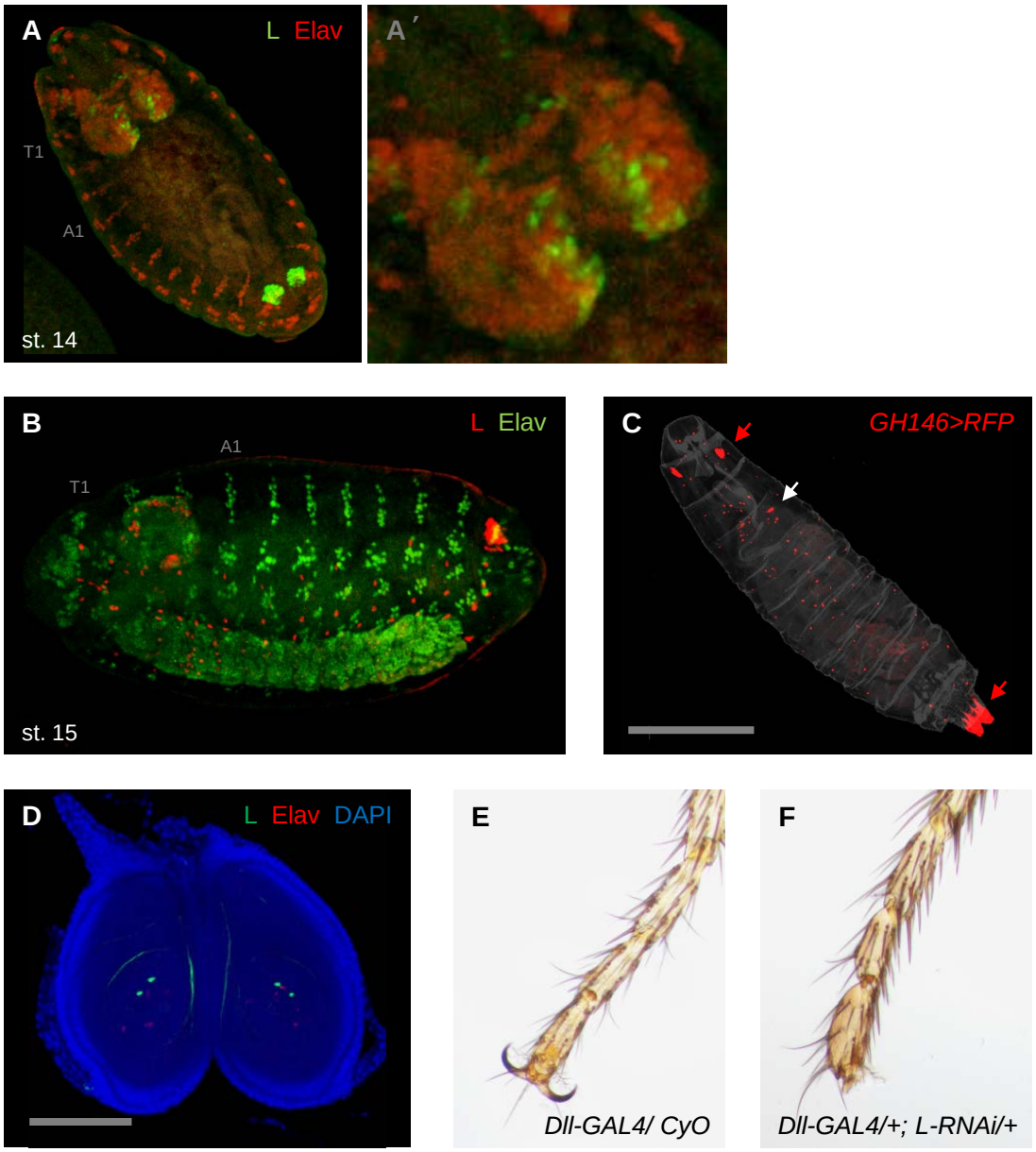
A
L Elav
T1
A1
st. 14
A′
B
L Elav
A1
T1
st. 15
C
GH146>RFP
D
L Elav DAPI
E
Dll-GAL4/ CyO
F
Dll-GAL4/+; L-RNAi/+
G
pro
meso
meta
Act-Cas9/+; U6-L-gRNA/+
*, missing claws

Figure S7. Endogenous L expression and mutational effects on claw formation.

The anti-L antiserum staining patterns by developmental stages were similar to the expression pattern of *L-GAL4* reporters (*P[GawB]GH146* and *P[GawB]NP5288*) during the embryonic and larval development. (A) L expression was detected in the dorso-posterior part of the embryonic brain and the posterior spiracles as reported previously (KRATTINGER *et al.* 2007). (B) In later stages, additional L expression was detected in a group of segmentally repetitive cells. (C) The embryonic expression appears to persist during larval development, in both anterior and posterior spiracles (red arrows) and in the larval hemisphere (white arrow) (see Figure S9). However, anti-L staining or *L-GAL4* activity was not detectable in the eye-antennal disc (Figure 6A, D) or other imaginal discs, except the leg disc. (D) L was detected in the distal end of the leg disc. (E, F) *L* RNAi by *Dll-GAL4* causes loss of distal structures. (G) Mutant clones generated by somatic CRISPR targeting at *L*. Only tarsal structures were affected during the leg development, consistent with specific L expressions in the distal part of the leg imaginal disc. Scale bars are 500 μm in (C) or 100 μm in (D).

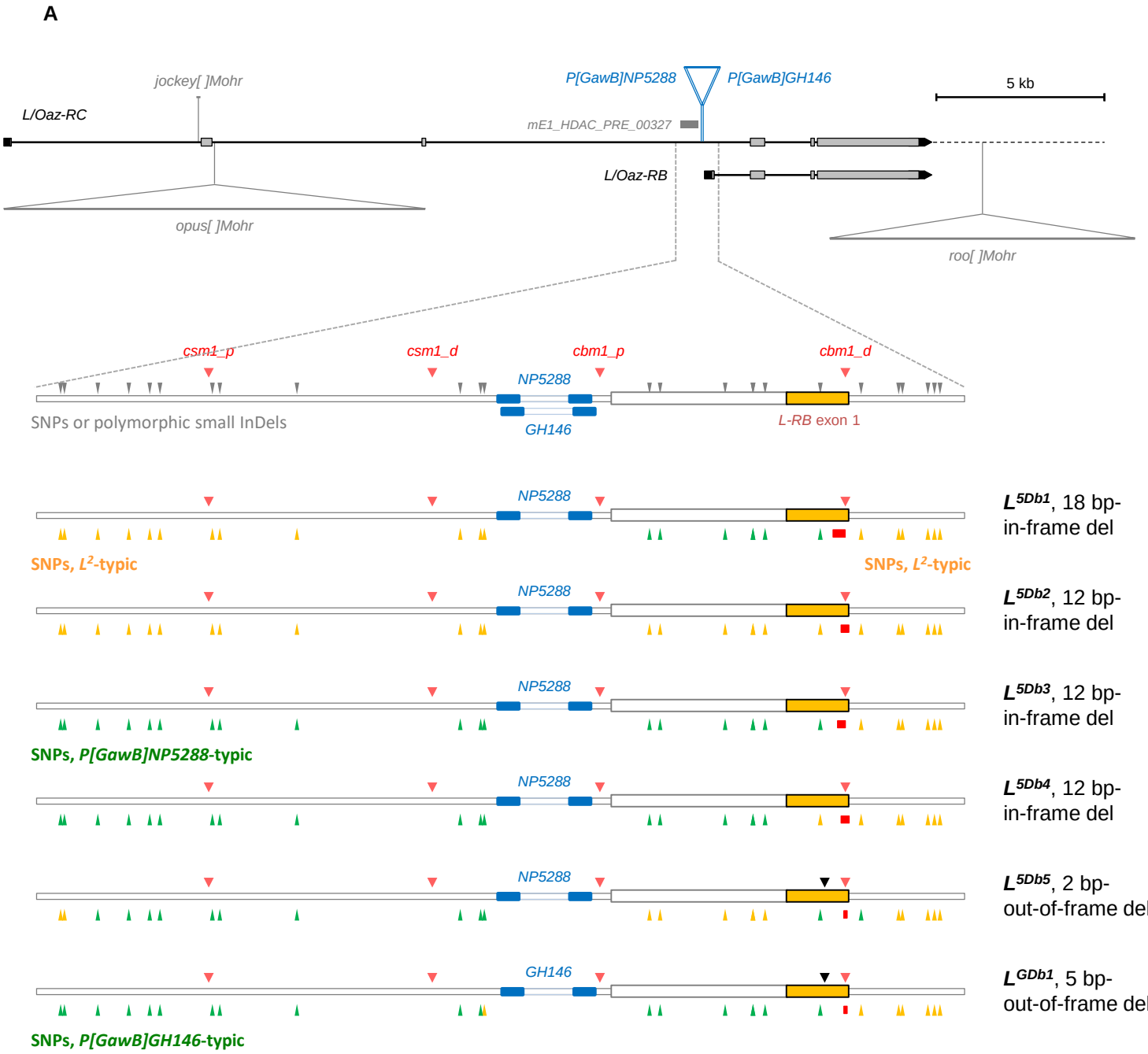

B

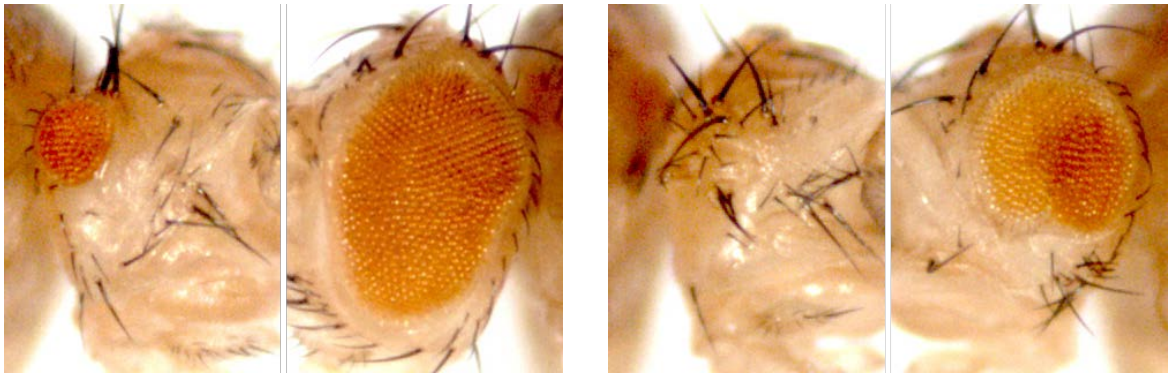

vas-Cas9/+; P[w+]BSC700/L2; U6-L-gRNA/+

vas-Cas9/+; PRAS40EY10689/L2; U6-L-gRNA/+

Figure S8. Recombination accompanied by CRISPR-targeting in the *L* region.

(A) Molecular maps of recombination sites between L^2 and its allelic *L-GAL4* insertions (*P[GawB]GH146* and *P[GawB]NP5288*, blue triangles). The L^2-specific mutations are located within the *roo[ ]Mohr* transposon (the rightmost gray triangle, see Figure 4C). By using the HR-dependent CRISPR targeting in the germline, homologous recombinants between these allelic mutations were collected to visualize ectopic *L-GAL4* activities due to L^2 mutation (Figure 6). Selected recombinant lines were analyzed by genomic sequencing, and origins of the recombined sequences were determined by polymorphic sequences between the *Mohr* strain (yellow for L^2,) and w^{1118} (green for *L-GAL4*s). CRISPR target sites are indicated by red color. All the analyzed distal sequences after the *cbm1 distal* site originated from the L^2 sequence, indicating that the 3'-located L^2 mutation was included in the recombinants. Red bars indicate short mutations in-frame or out-of-frame in the *L-RB* transcription, which were independently generated during the CRISPR targeting. (B) The Cas9 source under the *vasa* promoter used in this study for the germline expression (*M[vas-Cas9]ZH-2A*; (PORT *et al.* 2015) was also active in developing eye, thus generating frequent phenotypic mosaicism for L^2 mutation or w^{+m} expression.

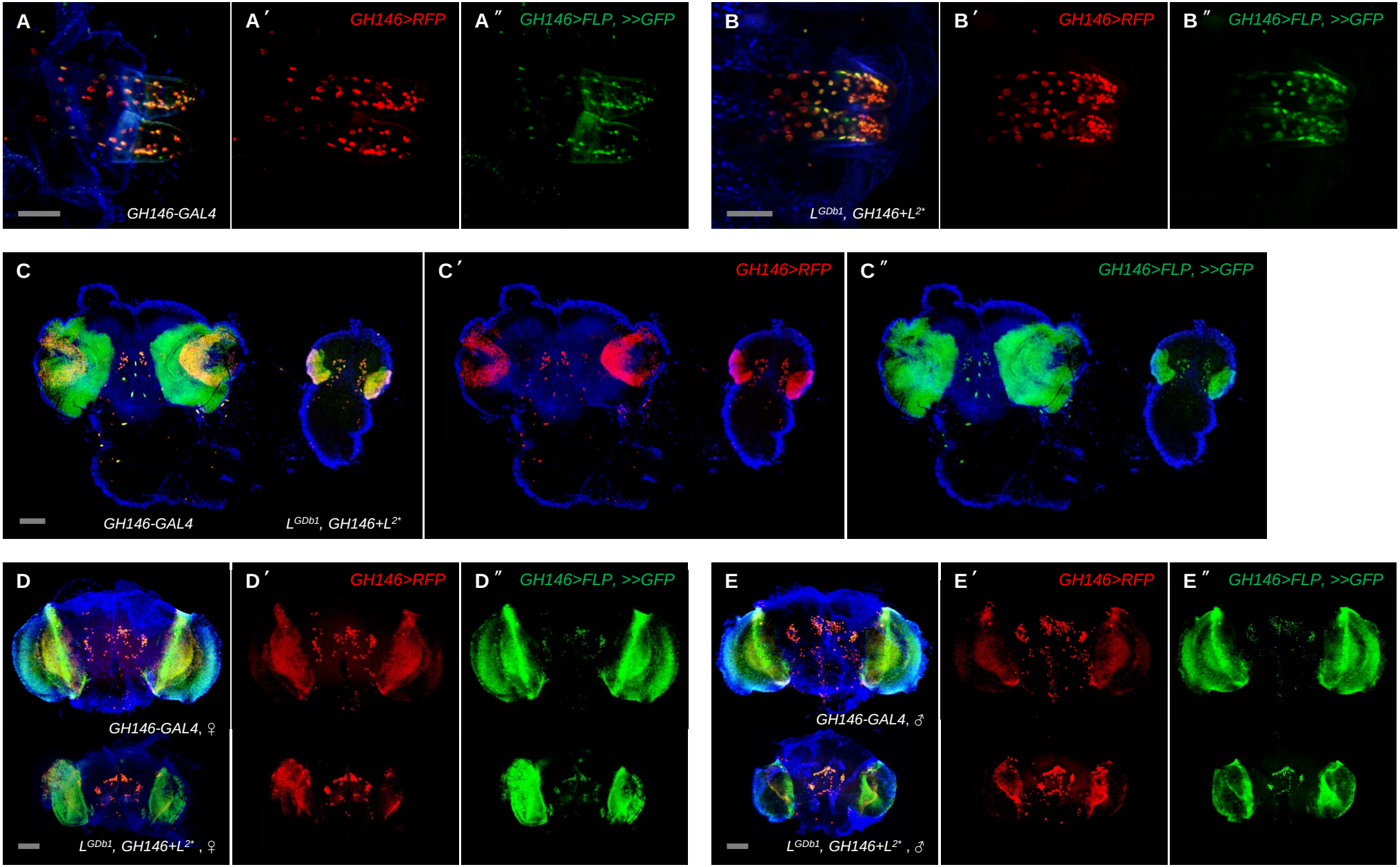
A
A′
GH146>RFP
A″
GH146>FLP, >>GFP
GH146-GAL4
B
B′
GH146>RFP
B″
GH146>FLP, >>GFP
L^GDb1, GH146+L^2*
C
C′
GH146>RFP
C″
GH146>FLP, >>GFP
GH146-GAL4
L^GDb1, GH146+L^2*
D
D′
GH146>RFP
D″
GH146>FLP, >>GFP
GH146-GAL4, ♀
L^GDb1, GH146+L^2* , ♀
E
E′
GH146>RFP
E″
GH146>FLP, >>GFP
GH146-GAL4, ♂
L^GDb1, GH146+L^2* , ♂

Figure S9. Effects of *L²* on *L-Gal4* expression in *cis*-recombinants.

L-GAL4 expression was examined in different tissues from *L-GAL4 L²* *cis*-recombinants: larval posterior spiracles (A, B), larval brain (C), and male and female adult brain (D, E). GAL4 activities were visualized by using the G-TRACE system (EVANS *et al.* 2009). Transheterozygotes between *L²*-recombined *L-GAL4* and the G-TRACE reporter (*L-GAL4 L²*/ *UAS-RFP, UAS-FLP, Ubi>>GFP*) showed abnormally delayed larval growth, producing only a few adult survivors of small body (small brains in C, D, E). However, real-time (*L-GAL4>RFP*) and clonal reporter expression (*L-GAL4>FLP, Ubi>>GFP*) in the *L²*-recombinants overlapped in general with those of the control *L-GAL4* drivers. Scale bars of 100 μm.

Constructed vectors	Target sequences	Targeting sites in the *L* region [a]
U6-DM1 *U6-DM2*	5’-ggtttcctgactgtgcgcac-agg-3’ 5’-gagggcattcggattgccac-cgg-3’	*L-RB* exon 4 (*L-RC* exon 6)
U6-cbm1	5’-gttattggtgatctccttgg-tgg-3’ 5’-gctctttggcactcggcctt-tgg-3'	*L-RB* exon 1 and promoter (distal to *L-GAL4* insertions)
U6-DE1	5’-tggatatatctttcggctag-agg-3’ 5’-agaccaaaacctgtggggca-agg-3’	*L-RC* intron 2, (flanking sides of *opus[ ]Mohr*)
U6-csm1	5’-gcctctgtgtgcgtgccttt-tgg-3’ 5’-gctggcgaagggcggagcat-ggg-3’	5’ to *L-RB* transcription (proximal to *L-GAL4* insertions)

Table S1. Guide RNA sequences used to target the *L* region.

[a)] The target sites in the *L* region are represented by arrowheads of different colors in Figure 5A, M and Figure S8A.

Genotype of transheterozygous F1 [a]	L^2 eye reversion in F2 by *U6-DE1* targeting [b]	L^2 eye reversion in F2 by *U6-cbm1* targeting [c]	L^2-recombinant with a homologous marker in F2 [d]	Homologous chromosome
L^2/SM6a	None (n>500)	1 revertant (n>500)	None (with *Cy*)	2nd chromosomal balancer
L^2/Sco	6 revertants (n>250)	-	15 recombinants with *Sco*	Different arm
L^2/PRAS40^{EY10689}	1 revertant (n>50)	1 revertant (n>150)	None (with w^{+m})	*P[w^{+m}]* located distal to *L*
L^2/Df(2R)BSC700,P[w^{+m}]	11 revertants (n>400)	17 revertants (n>250)	9 and 22 recombinants with w^{+m}, by *U6-DE1* and *U6-cbm1* targeting, respectively	Target sites present in the Df chromosome, *P[w^{+m}]* located proximal to *L*
L^2/Df(2R)Exel8059	2 revertants (n>500)	3 revertants (n>250)	*(no dominant homologous chromosomal marker)*	Target sites present in the Df chromosome
L^2/Df(2R)ED2354,P[w^{+m}]	None (n>500)	None (n>500)	None (with w^{+m})	Deficient in target sequences
L^2/Df(2R)BSC357	None (n>500)	-	*(no dominant homologous chromosomal marker)*	Deficient in target sequences
L^2/Df(2R)BSC668	None (n>300)	None (n>300)	*(no dominant homologous chromosomal marker)*	Deficient in target sequences

Table S2. CRISPR targeting in the *L* region with different homologous chromosomes.

[a)] Mutagenic F1 males carrying L^2 transheterozygous with the different homologous second chromosome (labelled 'II') were prepared (*vas-Cas9/Y; L^2/II; U6-L-gRNA/TM2*), and CRISPR mutagenesis efficacies in their germline were examined. Guide RNA transgenes of *U6-DE1* [b)] or *U6-cbm1* [c)] were used to target specific sites in the *L* region (Figure 5A). [d)] In addition to reversion from L^2 eyes, we also detected phenotypic recombination in males between L^2 and different homologous chromosomes in F1 transheterozygotes.

Supplementary References

EVANS, C. J., J. M. OLSON, K. T. NGO, E. KIM, N. E. LEE *et al.*, 2009 G-TRACE: rapid Gal4-based cell lineage analysis in Drosophila. Nat Methods **6:** 603-605.

HONG, W., M. NAKAZAWA, Y. Y. CHEN, R. KORI, C. R. VAKOC *et al.*, 2005 FOG-1 recruits the NuRD repressor complex to mediate transcriptional repression by GATA-1. EMBO J **24:** 2367-2378.

KRATTINGER, A., N. GENDRE, A. RAMAEKERS, N. GRILLENZONI and R. F. STOCKER, 2007 DmOAZ, the unique Drosophila melanogaster OAZ homologue is involved in posterior spiracle development. Dev Genes Evol **217:** 197-208.

LIN, A. C., A. E. ROCHE, J. WILK and E. C. SVENSSON, 2004 The N termini of Friend of GATA (FOG) proteins define a novel transcriptional repression motif and a superfamily of transcriptional repressors. J Biol Chem **279:** 55017-55023.

PORT, F., N. MUSCHALIK and S. L. BULLOCK, 2015 Systematic Evaluation of Drosophila CRISPR Tools Reveals Safe and Robust Alternatives to Autonomous Gene Drives in Basic Research. G3 (Bethesda) **5:** 1493-1502.

RYDER, E., F. BLOWS, M. ASHBURNER, R. BAUTISTA-LLACER, D. COULSON *et al.*, 2004 The DrosDel collection: a set of P-element insertions for generating custom chromosomal aberrations in Drosophila melanogaster. Genetics **167:** 797-813.

SINGH, A., X. SHI and K. W. CHOI, 2006 Lobe and Serrate are required for cell survival during early eye development in Drosophila. Development **133:** 4771-4781.